

# Cosmogenic $^3\text{He}$ ages and frequency of late Holocene debris flows from Prospect Canyon, Grand Canyon, USA

Thure E. Cerling <sup>a,\*</sup>, Robert H. Webb <sup>b</sup>, Robert J. Poreda <sup>c</sup>, Alan D. Rigby <sup>a</sup>,  
Theodore S. Melis <sup>d</sup>

<sup>a</sup> *Department of Geology and Geophysics, University of Utah, Salt Lake City, UT 84112, USA*

<sup>b</sup> *US Geological Survey, 1675 W. Anklam Road, Tucson, AZ 85745, USA*

<sup>c</sup> *Department of Geological Sciences, University of Rochester, Rochester, NY 14627, USA*

<sup>d</sup> *Grand Canyon Monitoring and Research Center, P.O. Box 22467, Flagstaff, AZ 86002, USA*

Received 18 May 1997; revised 12 March 1998; accepted 17 July 1998

---

## Abstract

Lava Falls Rapid, which was created and is maintained by debris flows from Prospect Canyon, is the most formidable reach of whitewater on the Colorado River in Grand Canyon and is one of the most famous rapids in the world. Debris flows enter the Colorado River at tributary junctures, creating rapids. The frequency of debris flows is an important consideration when management of regulated rivers involves maintenance of channel morphology. We used cosmogenic  $^3\text{He}$ ,  $^{14}\text{C}$ , and historical photographs to date 12 late Holocene and historic debris flows from Prospect Canyon. The highest and oldest deposits from debris flows on the debris fan yielded a  $^3\text{He}$  date of about 3 ka, which indicates predominately late Holocene aggradation of one of the largest debris fans in Grand Canyon. The deposit, which has a 25-m escarpment caused by river reworking, crossed the Colorado River and raised its base level by 30 m for an indeterminate although likely short period. We mapped depositional surfaces of 11 debris flows that occurred after 3 ka. Two deposits inset against the highest deposit yielded  $^3\text{He}$  ages of about 2.2 ka, and at least two others followed shortly afterwards. At least one of these debris flows also dammed the Colorado River. The most recent prehistoric debris flow occurred no more than 0.5 ka. The largest historic debris flow, which constricted the river by 80%, occurred in 1939. Five other debris flows occurred after 1939; these debris flows constricted the Colorado River by 35–80%. Assuming the depositional volumes of late Holocene debris flows can be modeled using a lognormal distribution, we calculated recurrence intervals of 15 to more than 2000 years for debris flows from Prospect Canyon. © 1999 Elsevier Science B.V. All rights reserved.

*Keywords:* cosmogenic isotopes; Grand Canyon;  $^3\text{He}$ ; geomorphology; Arizona; radiocarbon

---

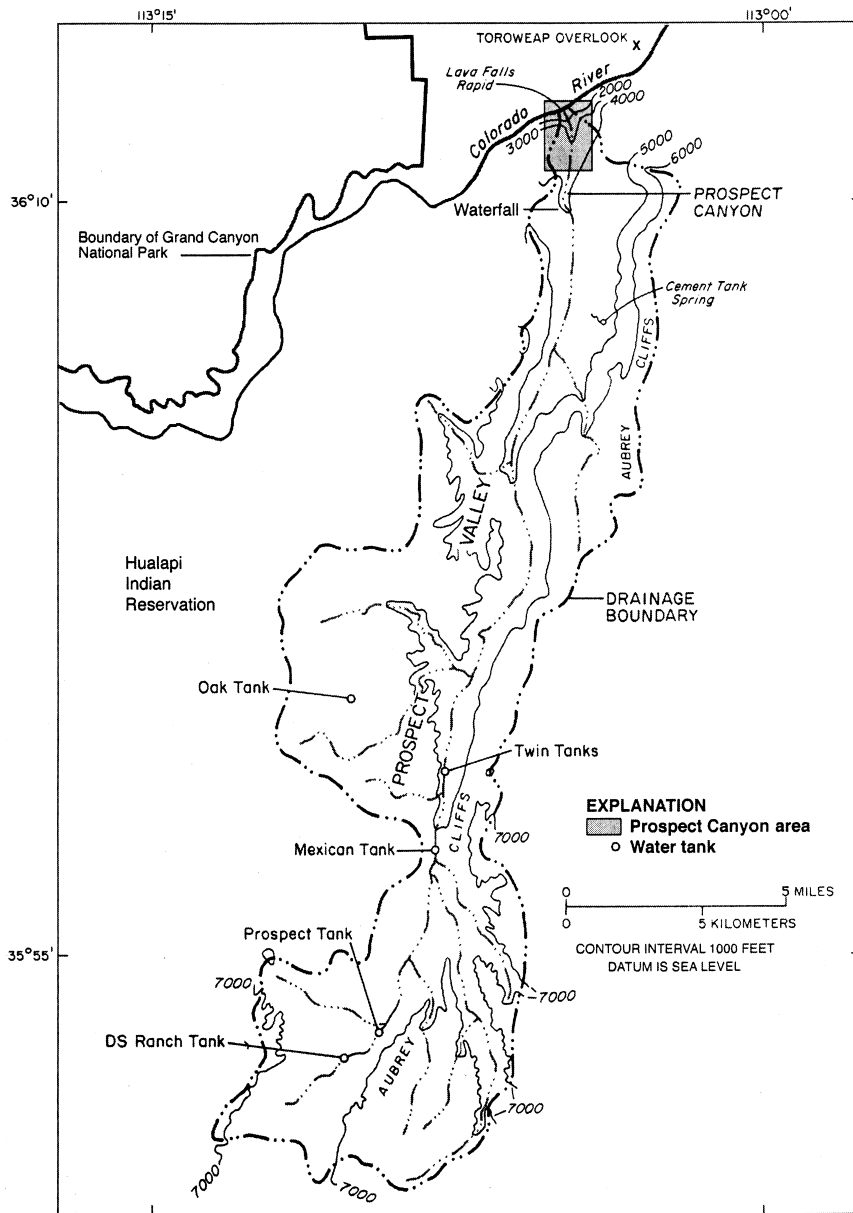
## 1. Introduction

Lava Falls Rapid, on the Colorado River in Grand Canyon (Fig. 1), is one of the most famous and

difficult navigable rapids in the continental United States (Nash, 1989). The rapid is at the mouth of Prospect Canyon at river mile 179.4, or 289 km downstream from Lees Ferry, Arizona (Stevens, 1990). Most of the rapids of the Colorado River, including Lava Falls, result from large boulders on

---

\* Corresponding author. E-mail: tcerling@mines.utah.edu



Base modified from U.S. Geological Survey 7.5' topographic maps, 1:24,000.

Fig. 1. Maps of the Prospect Valley drainage basin and Grand Canyon National Park.

debris fans at the mouths of tributary canyons (Hamblin and Rigby, 1968; Péwé, 1968; Simmons and Gaskill, 1969; Graf, 1979; Howard and Dolan, 1981; Kieffer, 1987, 1988) that were deposited by debris flows (Webb et al., 1988a, 1989; Melis et al., 1994). The Colorado River is a highly regulated river

whose channel morphology is modified by events adding debris to the channel. Maintenance of channel morphology is related to the frequency of these events. The debris fan at the mouth of Prospect Canyon, which creates Lava Falls, is one of the largest in Grand Canyon (Webb et al., 1996).

Debris flows are water-based slurries of poorly sorted sediments (Costa, 1984; Johnson and Rodine, 1984) that are a common component of flash floods in Grand Canyon (Webb et al., 1989; Melis et al., 1994). Steep slopes, such as the ones in Prospect Canyon, are a pre-requisite for the initiation of debris flows. The reported frequency of late Holocene debris flows varies widely in terrain not subjected to large-scale disturbances such as volcanic eruptions or forest fires. Debris flows may occur in discrete periods (Jackson, 1977; Hereford et al., 1996).

The typical frequency of debris flows in undisturbed terrain probably ranges from less than one per decade to about one per millennium (Jackson, 1977; Kochel, 1987; Osterkamp and Hupp, 1987; Shlemon et al., 1987; Lips and Wieczorek, 1990). Estimates of the frequency of debris flows from stratigraphic sections may underestimate the true frequency because of 'obliterative overlap' in which younger events bury older events (Gibbons et al., 1984). On the basis of photographic evidence, historic debris flows in Grand Canyon have a recurrence interval of 10–50 years in most tributaries (Melis et al., 1994; Webb, 1996). Some Grand Canyon tributaries have not had a debris flow in a 100-year photographic record (Webb, 1996), possibly for hydroclimatic reasons and (or) proximity to shale units (Griffiths et al., 1996). In contrast, debris flows in Warm Springs Draw in Dinosaur National Monument, Colorado, occur every 200–400 years (Hammack and Wohl, 1996).

Webb et al. (1996) report six debris flows in the 20th century from Prospect Canyon that substantially altered Lava Falls Rapid. The largest of these debris flows occurred in 1939 and constricted the river by 80%. Webb et al. (1996) also identified at least six late Holocene debris-flow surfaces. The largest debris flow, which occurred in about 1050 BC, is the best example of a debris flow that dammed the Colorado River in Grand Canyon during the late Holocene. Using only the historic debris flows and a 500-year-old event, Webb et al. (1996) estimated recurrence intervals of 20–200 years for debris flows in Prospect Canyon.

Measurement of in situ cosmogenic isotopes has recently been recognized as a technique to date geomorphic surfaces (Craig and Poreda, 1986; Klein et al., 1986; Lal, 1988; Cerling, 1990; Poreda and

Cerling, 1992; Cerling and Craig, 1994a; Cerling et al., 1994). The presence of abundant olivine phenocrysts in basalts in the Grand Canyon lava flows makes them suitable for study using cosmogenic  $^3\text{He}$ . The rate of production of cosmogenic  $^3\text{He}$  has been established (Cerling and Craig, 1994b) for the late Pleistocene to late Holocene, making feasible an extension of the cosmogenic  $^3\text{He}$  technique to late Holocene debris flows. In this study, we report  $^3\text{He}$  dates for the oldest surfaces on debris flows in Prospect Canyon and use them with conventional  $^{14}\text{C}$  dates and photographic evidence to estimate the frequency of the late Holocene debris flows that have affected Lava Falls Rapid.

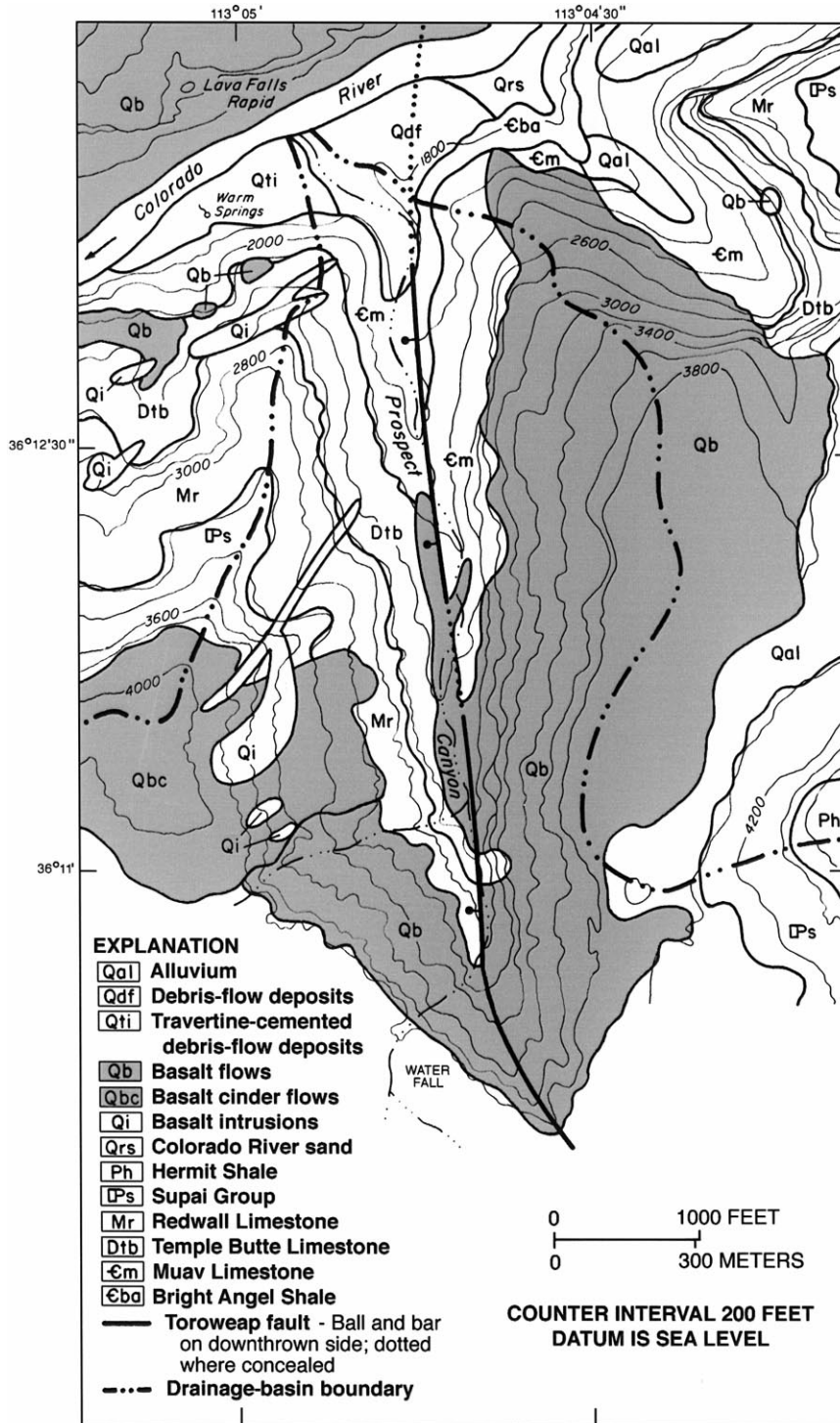
## 2. Methods

### 2.1. The Prospect Valley drainage basin

The Prospect Valley drainage basin consists of 257 km<sup>2</sup> of forest, grassland, and desert scrub south of Grand Canyon (Fig. 1) and is the ninth largest of 529 tributaries that produce debris flows in Grand Canyon (Melis et al., 1994). Most of the upper part of the drainage basin lies between 1450 and 1950 m. Prospect Valley drains northward and abruptly changes into a small gorge informally called Prospect Canyon (Fig. 2). The transition is a 325-m fall in a horizontal distance of approximately 250 m. The rocks exposed in Prospect Canyon consist of Paleozoic sedimentary strata and Quaternary basalts extruded from local vents (Fig. 2). The Toroweap Fault, which is downthrown to the west, trends south across the Colorado River (Billingsley and Huntoon, 1983; Jackson, 1990); Prospect Canyon formed along the fault axis.

Prospect Valley formed when Quaternary basalt flows filled the ancestral Prospect Canyon between 1.2 Ma and 140 ka (Hamblin, 1994). One of these flows also produced the Prospect Dam across the Colorado River (Hamblin, 1994). The modern Prospect Canyon occupies part of the former canyon, which joined the Colorado River upstream from the current mouth.

Debris flows in Prospect Canyon are generated when floods in Prospect Valley pour sufficient quantities of water over a 325-m near-vertical fall onto unconsolidated colluvium at its base, a process





from surveying data (Webb et al., 1996). This map (Fig. 3) delineates geomorphic surfaces, not stratigraphic units as depicted on other surficial geology maps of parts of Grand Canyon (Hereford, 1996). In addition to the detailed topographic information, latitude and longitude for  $^3\text{He}$  samples were measured using a hand-held geographical positioning system and also were mapped at the 1:2000 scale (Webb et al., 1996). Altitudes were determined by survey and are accurate to  $\pm 1$  m. Correction for shielding from canyon walls was made on the basis of measurements of horizon exposure from the sampling sites according to the method of Nishiizumi et al. (1989).

In general, the Prospect Canyon debris fan has two distinct types of debris-flow surfaces and several types of deposits related to other processes. The oldest and highest surfaces (Fig. 4) form the overall shape of the debris fan, and following Hereford et al. (1996) and Hereford (1996), we refer to these deposits as fan-forming debris-flow deposits. Subsequent channel incision gave rise to depositional sites for inset debris-flow deposits. Inset deposits are simi-

lar to those termed channelized debris flows by Hereford et al. (1996).

The ages of deposits on the Prospect Canyon debris fan are inherently difficult to determine in the absence of direct evidence such as photography (Webb et al., 1989). Although some researchers have abundant  $^{14}\text{C}$ -dated charcoal in debris-flow deposits because of forest fires (Meyer et al., 1995) or proximity to archaeological sites (Hereford et al., 1996), organic carbon is rare in most debris-flow deposits in Grand Canyon. We used age-dating techniques ranging from correlation of soil morphology to analysis of cosmogenic and radiometric isotopes. Several of these techniques—particularly  $^3\text{He}$  and  $^{14}\text{C}$  analyses—yielded absolute dates, whereas other techniques were used to establish relative ages or to distinguish or correlate discontinuous deposits.

### 2.3. Absolute and relative age-dating techniques

The basalt clasts in Prospect Canyon debris flows contain olivine phenocrysts (Hamblin, 1994), which



Fig. 4. View of the Prospect debris fan on March 7, 1995 (photograph by S. Tharnstrom). Surface tfa dominates the left center of the view. Deposition from the 1995 debris flow appears at right center adjacent to the rapid.

are efficient traps for cosmogenically produced helium, termed  $^3\text{He}_c$  (Craig and Poreda, 1986; Kurz, 1986; Cerling, 1990; Cerling and Craig, 1994a). The samples were collected from a relatively small area on the Prospect Canyon debris fan (Table 1, Fig. 3). Samples for in situ cosmogenic  $^3\text{He}$  studies were chosen that were at least 1 m in diameter (Fig. 5). All samples had abundant phenocrysts with few vesicles, which indicate that they were derived from the interior of the respective lava flows. The upper 4 cm was crushed and sieved to less than 20 mesh. Olivine separates were prepared by magnetic separation, heavy liquids, and hand-picking. Samples were crushed under high vacuum to release mantle helium contained in inclusions for separate analyses.

Powders and uncrushed phenocrysts were melted at 1800°C in a modified Turner-type furnace, and the liberated gas was purified using getters and cryogenic traps. Isotope measurements were made on a VG 5400 mass spectrometer fitted with electron multiplier and pulse counting electronics.  $^3\text{He}/^4\text{He}$  ratios were standardized against the SIO-MM standard at 16.45  $R_a$  (where  $R_a$  is the atmospheric

$^3\text{He}/^4\text{He}$  ratio). All values were corrected for interference peaks, instrumental and extraction blanks (Poreda and Cerling, 1992; Poreda and Farley, 1992).

Corrections were made for contamination, radiogenic  $^4\text{He}$ , and local shielding.  $^4\text{He}$ ,  $R/R_a$  (melt), and  $R/R_a$  (crush) were corrected for air contamination using measured  $^{22}\text{Ne}$  concentrations, assuming that all  $^{22}\text{Ne}$  was from air. Samples were corrected for the mantle component of  $^3\text{He}$  using the  $R/R_a$  value determined from crushed phenocrysts. Occasionally, crush values gave  $R/R_a$  ratios  $< 1$  indicating contamination of a highly radiogenic component. If after correction for blanks and air contamination the  $R/R_a$  ratio was lower than the crush value, we assumed that the residual  $^4\text{He}$  was radiogenic. Background values for  $^3\text{He}$  and  $^4\text{He}$  are  $13,500 \pm 5,000$  atoms and 0.1 ncc ( $10^{-9}$  cc at STP), respectively, and hot blank values for  $^3\text{He}$  ranged between 0.01 and  $0.07 \times 10^6$  atoms per run over the two-year period of analysis.  $^3\text{He}_c$  values were corrected to the surface ( $z = 0$ ), and local rates of production at  $z = 0$  were corrected for skyline shielding ( $P *_{z=0}$ ) using the relation of Nishiizumi et al. (1989). Repli-

Table 1

Sample data for basalt clasts collected for cosmogenic  $^3\text{He}$  dating from the Prospect Canyon debris fan

Sample number	Latitude (N)	Longitude (W)	Elevation (m)	$P_{z=0}$ (at $\text{g}^{-1} \text{ year}^{-1}$ )	Shielding factor	$P *_{z=0}$ (at $\text{g}^{-1} \text{ year}^{-1}$ )
<i>Surface tfa</i>						
93 LVA FLS 1	36.1982	113.0800	552	166.1	0.913	151.6
93 LVA FLS 4	36.1970	113.0793	556	166.6	0.913	152.1
93 LVA FLS 6	36.1965	113.0798	559	167.0	0.913	152.5
93 LVA FLS 8	36.1965	113.0798	550	165.8	0.913	151.4
93 LVA FLS 9	36.1943	113.0814	561	167.3	0.820	137.2
93 LVA FLS 12	36.1943	113.0814	562	167.5	0.820	137.3
93 LVA FLS 14	36.1967	113.0803	551	165.9	0.744	123.5
93 LVA FLS 15	36.1967	113.0803	551	165.9	0.744	123.5
<i>Surface tia</i>						
93 LVA FLS 24	36.1974	113.0808	536	163.9	0.828	135.7
93 LVA FLS 25	36.1974	113.0808	536	163.9	0.828	135.7
<i>Surface tib</i>						
93 LVA FLS 22	36.2000	113.0817	542	164.7	0.809	133.3
93 LVA FLS 23	36.2000	113.0817	542	164.7	0.809	133.3
<i>Surface tig (AD 1939)</i>						
93 LVA FLS 16	36.1973	113.0823	522	162.0	0.780	126.4
93 LVA FLS 17	36.1973	113.0823	522	162.0	0.780	126.4
93 LVA FLS 18	36.1973	113.0823	522	162.0	0.780	126.4

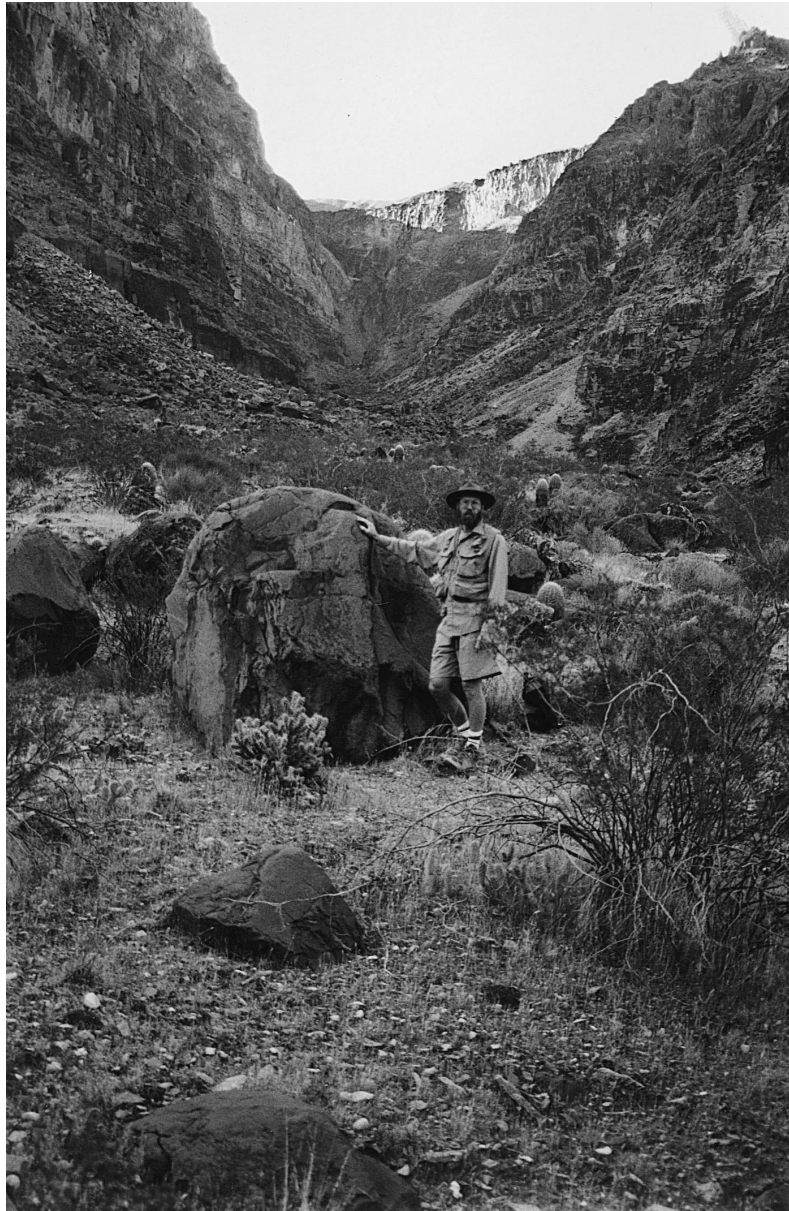


Fig. 5. Large boulder deposited on surface tfa that was sampled for a cosmogenic  $^3\text{He}$  date (photograph by A. Rigby).

cate samples of  $^3\text{He}$  from the well-dated Tabernacle Hill basalt (17.4 ka) yield 6.2 million atoms  $\text{g}^{-1}$ ; our calibration is based on a high latitude ( $> 60^\circ$ ) and sea level  $^3\text{He}_c$  rate of production of 115 atoms  $\text{g}^{-1} \text{year}^{-1}$  (Cerling and Craig, 1994a,b). No corrections were made for changes in the  $^3\text{He}_c$  rate of production because of changes in secular variation or in the

strength of the magnetic field of Earth because accurate data are not available. Samples dated by  $^{14}\text{C}$  from the nearby Zuni volcanic field have  $^3\text{He}_c$  rates of production (unpublished data, manuscript in preparation) very similar to that measured by Cerling and Craig (1994a,b) when corrected to sea level and high latitude. Age is given as the absolute age in ka,

calculated from calibrated  $^{14}\text{C}$  years BP. Sample localities and shielding information are given in Table 1.

We used radiocarbon ( $^{14}\text{C}$ ) analyses to date some debris flow-deposits on the Prospect Canyon debris fan. We collected various types of organic debris, including pieces of driftwood and small twigs, from the top of several debris-flow surfaces. The 'best' samples appeared to be fine-grained organic debris (e.g., small twigs) wrapped around or pinned beneath cobbles and boulders in debris-flow levees. No organic material was observed at depth in the debris-flow deposits or on the oldest debris-flow surfaces. The resulting radiocarbon dates were converted to calendar ages using computer routines (Stuiver and Becker, 1993; Stuiver and Reimer, 1993).

The soil on the oldest surfaces is weakly developed, but contains pedogenic calcium carbonate, which reflects the age of the soil and the underlying deposit (Birkeland, 1984). The greatest accumulation of  $\text{CaCO}_3$  in the soil on the Prospect Canyon debris fan is Stage I carbonate morphology (see Machette, 1985, for a description of carbonate stages) with a maximum accumulation at about 0.50 m depth. In hot desert soils, this amount of accumulation generally occurs in surfaces deposited in the latest Pleistocene or Holocene (Table 2 in Machette, 1985). Hereford et al. (1996) also used soil carbonate to differentiate the ages of debris flows in Grand Canyon.

Desert vegetation on the Prospect Canyon debris fan was used to estimate relative ages of surfaces. Webb et al. (1987, 1988b) and Bowers et al. (1998) showed that the species composition of desert vegetation on debris-flow deposits is related to the age of the deposit. Creosote bush (*Larrea tridentata*) forms clonal rings (Vasek, 1980) that are indicative of the age of the surface that the plant is growing on. As a creosote bush ages, the center of the root crown dies and the outer segment of the root crown splits into genetically identical clones. The ring that forms continues to expand radially at the average rate of  $0.66 \text{ mm yr}^{-1}$  (Vasek, 1980). The diameter of a creosote bush clonal ring, therefore, reflects the establishment date for the plant and gives a minimum age for the surface on which it is growing. The uncertainty on the clonal ring data is on the order of  $\pm 20\%$  which includes the variability from three different sites,

from a region where the climate is similar to that of Prospect Canyon.

#### 2.4. Surface area, volume, and constrictions

The area and volume of sediment deposited by late Holocene debris flows was estimated using slope projection on the 1:2000 scale maps. From the remnant deposits, we projected the slope of the deposit toward the Colorado River until its projected elevation either intersected the profile of the water-surface of the river at a stage corresponding to  $140 \text{ m}^3 \text{ s}^{-1}$  (the flow when our aerial photographs were taken during our base line surveys) or reached the right bank. We then used the projected slope to estimate the areal extent of deposition and constriction of the Colorado River; all surfaces were projected over the 1993 debris fan and Lava Falls Rapid. We estimated average thicknesses of debris fans (Melis et al., 1994; Webb et al., 1996) and calculated the depositional volume as the product of area and average thickness.

Historic debris flows from Prospect Canyon constricted the Colorado River substantially at Lava Falls Rapid. The percentage constriction,  $C$ , is expressed as:

$$C = \left[ 1 - 2W_{r(\text{ave})} / (W_u + W_d) \right] 100\%,$$

where  $W_{r(\text{ave})}$  is the average width of the constricted channel in the rapid,  $W_u$  is the upstream width of the Colorado River, and  $W_d$  is the downstream width of the rapid below the expansion zone. For the maximum  $C$ ,  $W_{r(\text{ave})}$  is the narrowest width of the rapid. Because river banks typically are steep upstream and downstream from the rapid, and because the surface of the debris fan typically has a relatively low slope angle,  $C$  increases as the discharge decreases below the point where a significant area of the debris fan is exposed. For this reason, values of  $C$  are for a discharge of about  $140 \text{ m}^3 \text{ s}^{-1}$  which was the flow when our aerial photographs were taken.

#### 2.5. Frequency

We used the volumes of debris flows from Prospect Canyon to estimate recurrence intervals. We assumed that oblitative overlap (Gibbons et al., 1984) is not a factor in the preservation of debris

Table 2  
Analytical data for basalt samples from the Prospect Canyon debris fan in Grand Canyon

Sample number	$^3\text{He}$ blank (%)	$^4\text{He}$ (ncc $\text{g}^{-1}$ )	$R/R_a$ melt	$R/R_a^a$ crush	$^3\text{He}_c$ (%)	$^3\text{He}_c$ ( $10^6$ at $\text{g}^{-1}$ )	$^3\text{He}_c$ ( $z=0$ ) ( $10^6$ at $\text{g}^{-1}$ )	$P^*_{z=0}$ (at $\text{g}^{-1}$ year $^{-1}$ )	Age (ka $\pm$ uncertainty)
<i>Surface tfa</i>									
LVA FLS 01	11.2	1.97	12.0	5.5	47.0	$0.481 \pm 0.063$	$0.500 \pm 0.065$	152	$3.30 \pm 0.43$
LVA FLS 01	2.0	2.59	8.1	5.5	31.6	$0.254 \pm 0.041$	$0.264 \pm 0.042$	152	$1.74 \pm 0.28^b$
LVA FLS 04	9.1	1.59	7.0	5.5	83.9	$0.416 \pm 0.031$	$0.433 \pm 0.032$	152	$2.84 \pm 0.21$
LVA FLS 06	6.7	0.31	78.6	5.5	85.2	$0.859 \pm 0.050$	$0.893 \pm 0.051$	153	$5.86 \pm 0.34^b$
LVA FLS 06	2.9	1.41	11.0	5.5	49.2	$0.294 \pm 0.035$	$0.306 \pm 0.036$	153	$2.01 \pm 0.24$
LVA FLS 08	4.2	0.48	51.6	5.5	83.6	$0.821 \pm 0.045$	$0.854 \pm 0.047$	151	$5.64 \pm 0.31^c$
LVA FLS 09	13.5	1.11	14.6	5.5	48.5	$0.378 \pm 0.058$	$0.506 \pm 0.049$	137	$3.69 \pm 0.36$
LVA FLS 12	12.8	0.37	30.9	5.5	69.2	$0.353 \pm 0.030$	$0.367 \pm 0.031$	137	$2.67 \pm 0.23$
LVA FLS 14	8.9	3.09	3.7	5.5	83.1	$0.425 \pm 0.033$	$0.442 \pm 0.034$	124	$3.58 \pm 0.28$
LVA FLS 15	2.8	0.88	15.8	5.5	61.0	$0.339 \pm 0.032$	$0.353 \pm 0.033$	124	$2.86 \pm 0.27$
LVA FLS 15	14.7	1.46	11.7	5.5	65.0	$0.342 \pm 0.039$	$0.356 \pm 0.040$	124	$2.88 \pm 0.33$
LVA FLS 15	11.1	0.48	50.2	5.5	76.3	$0.812 \pm 0.065$	$0.844 \pm 0.067$	124	$6.84 \pm 0.55^b$
<i>Surface tia</i>									
LVA FLS 24	18.8	1.58	3.9	5.5	81.1	$0.232 \pm 0.027$	$0.241 \pm 0.028$	136	$1.78 \pm 0.21$
LVA FLS 25	13.9	1.91	4.8	5.5	85.8	$0.341 \pm 0.030$	$0.355 \pm 0.031$	136	$2.61 \pm 0.23$
<i>Surface tib</i>									
LVA FLS 22	17.3	0.98	6.7	5.5	73.2	$0.244 \pm 0.029$	$0.254 \pm 0.030$	133	$1.90 \pm 0.23$
LVA FLS 23	26.9	0.13	70.1	5.5	63.7	$0.314 \pm 0.054$	$0.327 \pm 0.056$	133	$2.45 \pm 0.42$
<i>Surface tig (1939)</i>									
LVA FLS 16	40.1	0.12	19.3	5.5	48.7	$0.084 \pm 0.030$	$0.087 \pm 0.031$	126	$0.69 \pm 0.25$
LVA FLS 17	21.6	0.92	5.2	5.5	65.0	$0.180 \pm 0.025$	$0.187 \pm 0.026$	126	$1.48 \pm 0.21$
LVA FLS 18	54.4	2.15	0.9	5.5	36.6	$0.077 \pm 0.048$	$0.080 \pm 0.050$	126	$0.63 \pm 0.40$

<sup>a</sup>Crush value of 5.5 is the average for three different samples from the debris fan.

<sup>b</sup>Data rejected on the basis of choice of duplicate sample.

<sup>c</sup>Data possibly should be rejected because its value is high.

<sup>4</sup>He and  $R/R_a$  are the measured values and do not have blank or air corrections applied. Uncertainty estimates include all analytical precision uncertainties in the measurements, and do not include uncertainties in altitude-latitude scaling or in uncertainties in the production rate.

Age is given as the absolute age (ka from calibrated  $^{14}\text{C}$  years BP).

flows in the late Holocene. Also, we assumed the frequency of debris-fan production at the mouth of Prospect Canyon could be approximated using a lognormal distribution. Because debris fans do not form every year, and years with zero volume are difficult to model using log-transformed data (Kite, 1988), we chose a minimum censoring threshold volume of 3000 m<sup>3</sup>, which also minimizes the effects of obliterative overlap of the smallest debris flows. We then used a maximum-likelihood procedure (Stedinger and Cohn, 1986; Stedinger et al., 1988) to fit a lognormal distribution to the volume data.

### 3. Results

#### 3.1. Surficial geology of the Prospect Canyon debris fan

The Prospect Canyon debris fan has a plan area of 9.2 ha and a volume of 1.9 million m<sup>3</sup> above the 140 m<sup>3</sup> s<sup>-1</sup> stage of the Colorado River. The surficial deposits on the Prospect Canyon debris fan are poorly sorted mixtures with sizes from clay to boulders (Webb et al., 1996). Between 40 and 63% of the clasts in debris flows from Prospect Canyon are Pleistocene basalt (Webb et al., 1996). The reason for the abundance of basalt is the large amount of Pleistocene basalt in Prospect Canyon, especially in the vicinity of the waterfall (Fig. 2).

##### 3.1.1. Surface tfa

The highest surface on the Prospect Canyon debris fan, surface tfa, is underlain by late-Holocene, fan deposits formed by debris flows. The area of this surface, the largest on the debris fan, is 4.38 ha. Although individual lobes and snouts have surface expressions on surface tfa, the surficial deposits appear to be of uniform age. The surface is about 15 m above the channel of Prospect Canyon and 25 m above the Colorado River at its maximum height (Webb et al., 1996). Three distinct strata appear in the vertical exposures, each of which represents deposition by an unknown number of debris flows. No soil is recognized at the top of the lower strata, which suggests that deposition of the main body of the debris fan occurred at a faster rate than soil-forming processes.

We analyzed <sup>3</sup>He<sub>c</sub> concentrations in olivine phenocrysts in 15 samples from eight basalt boulders on surface tfa (Table 2). For such young samples collected at low elevations, with the added complication of shielding from the canyon walls, we identified some complications that would not be apparent in older samples with more abundant cosmogenic <sup>3</sup>He<sub>c</sub>. Surface tfa, for which we have the most analyses, illustrates this well. Crushing the olivines releases <sup>3</sup>He and <sup>4</sup>He which represent the original <sup>3</sup>He/<sup>4</sup>He ratio at the time of eruption. Addition of cosmogenic <sup>3</sup>He increases the <sup>3</sup>He/<sup>4</sup>He ratio, so that the melt <sup>3</sup>He/<sup>4</sup>He ratios are higher than the crush values. Normally, the crush value is used to correct the melt value for any residual 'original' <sup>3</sup>He. Addition of a small amount of radiogenic <sup>4</sup>He (i.e., by implantation; Lal et al., 1989), however, would reduce the <sup>3</sup>He/<sup>4</sup>He ratio and would mean that an overcorrection is made and would result in very low <sup>3</sup>He<sub>c</sub> values. For this suite of samples, some of the splits had *R/R<sub>a</sub>* ratios for the melt that were lower than the crush values when corrected for the blank and air contributions (in one case, *R/R<sub>a</sub>* (melt) < 1.0), which is indicative of a radiogenic <sup>4</sup>He component (e.g., sample 14 from tfa; samples 24 and 25 from tia; samples 17 and 18 from tig). Because the correction for inherited <sup>3</sup>He is based on the measured <sup>4</sup>He concentration, this introduces some uncertainty into the analysis. For the samples in this study, the maximum difference in the calculated concentration of cosmogenic <sup>3</sup>He was 0.3 × 10<sup>6</sup> at g<sup>-1</sup> or less. An uncertainty of this magnitude would be small for old samples, but is significant in this study where the total <sup>3</sup>He<sub>c</sub> is on the order of 0.5 × 10<sup>6</sup> at g<sup>-1</sup> or less.

The 12 analyses from surface tfa yielded an average <sup>3</sup>He<sub>c</sub> age of 3.6 ka (Table 2). Of these analyses, seven yielded <sup>3</sup>He<sub>c</sub> ages between 2.6 and 3.6 ka; two analyses gave younger ages and three yielded older ages (Fig. 6). Several of the replicate analyses showed significantly older or younger dates than the remainder for the same boulder; for example, for sample 15, we obtained <sup>3</sup>He<sub>c</sub> ages of 2.86, 2.88, and 6.84 ka (Table 2), which suggests that the 6.84 ka date should be discarded. Eliminating the three incongruous duplicate samples (two high, one low; Table 2), we obtained a date of 3.3 ± 1.0 ka. For sample 8, we obtained an age of 5.64 ka with no duplicate, and eliminating this analysis yielded an average age of

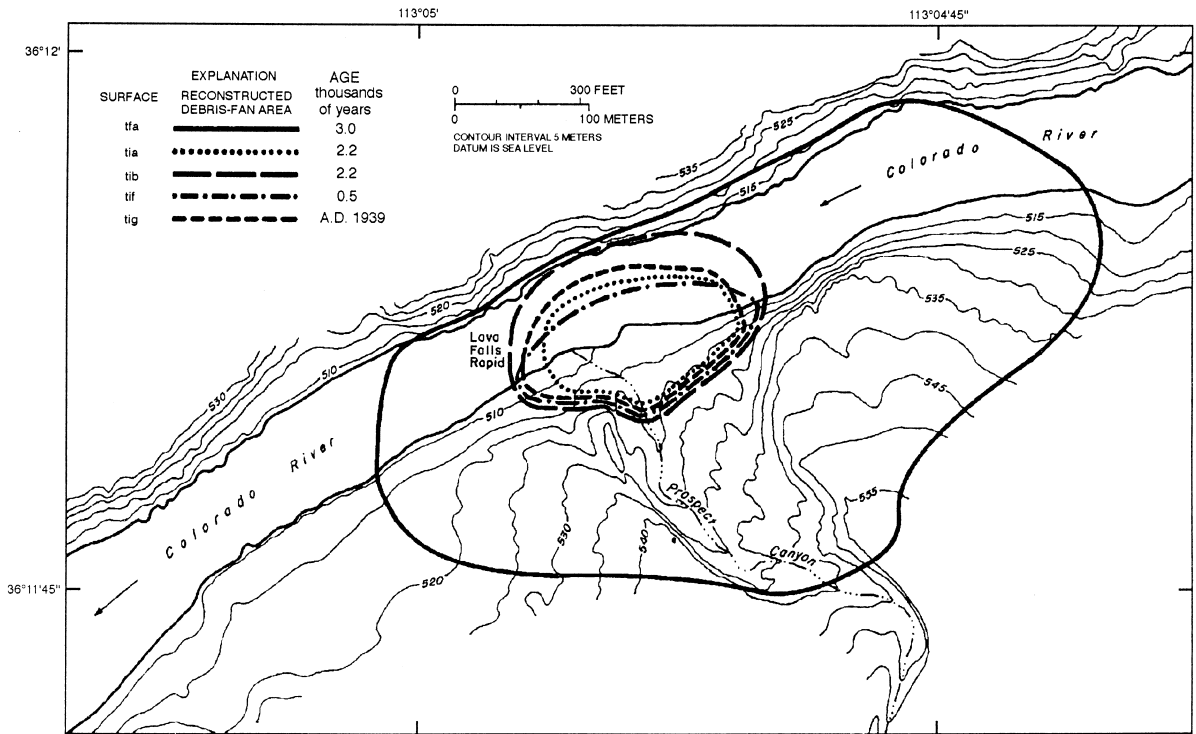


Fig. 6. The spatial extent of debris fans deposited by Holocene debris flows from Prospect Canyon. The location of the edge and the thickness of the debris fan were determined by projection into the river from remnant deposits.

$3.0 \pm 0.5$  ka. Given these uncertainties, we believe that the most parsimonious estimate of the cosmogenic exposure age of surface tfa is about 3.0 ka, which we consider to be the maximum age of the surface of the debris fan.

The soil on surface tfa has a thin and weakly developed A horizon, stage I carbonate accumulations on particles with a maximum at 0.50 m depth, and no cambic development in the profile. Such soil profile is indicative of a Holocene deposit (Machette, 1985). The Toroweap Fault (Fig. 2) crosses the Prospect Canyon debris fan without a surface rupture (Jackson, 1990). Using soil pedogenic features, Jackson (1990) estimated a 3.1 ka age for the most recent rupture in Prospect Valley. Other relative age-dating techniques generally agree with this age. Creosote bush growing on this surface forms distinct clonal ring-structures between 1.02 and 1.35 m in diameter. Using the relation of Vasek (1980), the plants were established between 1.4 and 1.9 ka, which is a minimum age for surface tfa.

### 3.1.2. Surface tia

Surface tia is a triangular-shaped remnant of a debris-flow levee and is the oldest of the inset debris-flow surfaces on the Prospect Canyon debris fan. The surface, which has an area of 800 m<sup>2</sup>, is underlain by poorly sorted deposits with occasional boulders that have fallen from surface tfa. The larger particles are subangular to rounded clasts of moderately varnished basalt and moderately weathered limestone and sandstone.

<sup>3</sup>He<sub>c</sub> concentrations in olivine phenocrysts in two basalt samples from surface tia (Table 2) indicate an age of  $2.2 \pm 0.6$  ka. The selection of boulders for cosmogenic work on surface tia is more limited than on surface tfa because the fan area is much smaller and potential exists for contamination by boulders fallen from surface tfa. We avoided boulders that appeared to be talus and only collected two boulders from surface tia; hence, the uncertainty in the cosmogenic age may be much greater than indicated by statistics. The <sup>3</sup>He<sub>c</sub> age is younger than surface tfa,

which is in accord with the inset stratigraphic relation between the two surfaces.

The soil underlying surface tia has a weak A horizon and Stage I carbonate on clasts similar to surface tfa. Maximum development of carbonate is at 0.50 m; below a depth of 1.0 m, carbonate coatings on clasts are very weak. The vegetation is mostly creosote bush with scattered shrubs and barrel cacti; the creosote bush clonal rings range in diameter from 0.60 to 1.50 m, which corresponds to an establishment age of 0.8 to 2.2 ka.

### 3.1.3. Surface tib

Surface tib, with an area of 0.28 ha, is the largest of the inset surfaces of Prospect Canyon and is inset against surfaces tfa and tia (Fig. 3). An internal drainage channel bisects the surface into eastern and western segments. Sediment is poorly sorted with boulders up to 3 m in diameter, and larger boulders that fell from surface tfa also lie on the surface.

$^3\text{He}_c$  concentrations in olivine phenocrysts in basalt on surface tib indicate an age of  $2.2 \pm 0.4$  ka. As with surface tia, the selection of boulders for cosmogenic  $^3\text{He}_c$  analyses is more limited than on surface tfa because the fan area is much smaller and there is evidence for contamination by boulders fallen from surface tfa. We selected two boulders that could not have fallen from surface tfa based on their relative positions. The  $^3\text{He}_c$  age of surface tib is younger than surface tfa and equal to the age of surface tia. Based on the geometry of the surfaces, surface tib is younger than surfaces tfa or tia.

Clasts are weathered and varnished slightly less than similar clasts on surface tia and some of these clasts appear to have faint percussion marks that occurred during transport in a debris flow. The soil has a weakly developed A horizon and Stage I carbonate that is similar to the development of soil on tia. Creosote bush dominates the plant assemblage, and most of the shrubs appear to be in clonal rings that range between 0.10 and 0.60 m in diameter. These rings suggests that the creosote bushes became established between 0.1 to 0.8 ka.

### 3.1.4. Surfaces tic, tid, and tie

Surfaces tic, tid, and tie are push-out lobes onto surface tib and occupy 314 m<sup>2</sup> near the apex of the

Prospect Canyon debris fan (Webb et al., 1996). We consider surface tic to represent one debris flow and surfaces tid and tie to represent a second event. The development of soil and weathering of clasts on these surfaces are of similar age to surfaces tia and tib. Several creosote bushes dominate the vegetation on these small surfaces and form clonal rings 0.30 to 0.50 m in diameter, which suggests an establishment age between 0.4 and 0.6 ka. We did not find boulders acceptable for  $^3\text{He}$  cosmogenic dating on these surfaces.

### 3.1.5. Surface tif

Sediments from debris flows underlie the prominent surface tif in a 0.18-ha area along the east side of Prospect Canyon (Fig. 3) and on the downstream side of Lava Falls Rapid. Driftwood collected from under cobbles on surface tif yielded a radiocarbon age of  $0.485 \pm 0.09$  ka, which corresponds to a calendar date range of (AD 1296–1640) (Table 3). A date of AD 1434, based on  $^{14}\text{C}$  measurements, represents the maximum age of this debris flow. Snouts and boulder-strewn levees are prominent on this jumbled surface, and about 49% of the clasts are basalt and 35% are limestone. Boulders are lightly varnished, and prominent percussion marks reflect the young age of this surface. The absence of creosote bushes on this surface indicates a young age (Bowers et al., 1998).

### 3.1.6. Surface tig

Deposits from the 1939 debris flow form the extensive surface tig that is inset against older deposits on both sides of Prospect Canyon. Levee deposits on both sides have a maximum thickness of about 4 m and an area of 0.65 ha. Sixty-two percent of the clasts on surface tig are basalt, the highest amount of basalt of any of the debris flows from Prospect Canyon (Webb et al., 1996). Creosote bushes are absent from this surface.

$^3\text{He}_c$  ages for boulders from surface tig are several hundred years old, averaging  $0.9 \pm 0.5$  ka. The  $^3\text{He}$  blank correction, however, is up to 50% of total measured  $^3\text{He}$ , a much higher blank correction than was associated with the other boulders from surfaces tfa, tia, and tfb. The samples from this young flow limit the resolution of the  $^3\text{He}$  cosmogenic dating

Table 3

Radiocarbon dates of organic material collected from debris-flow deposits at the mouth of Prospect Canyon

Surface (date)	Sample number	Type of organic material	Radiocarbon date (ka $\pm$ 1 $\sigma$ or PMC)	Calendar date (AD)	2 $\sigma$ range in date (AD)
tif	GX-19925	wood	0.485 $\pm$ 0.09	1434	1296–1640
tig (1939)	GX-19326	wood	0.460 $\pm$ 0.075	1439	1327–1638
tih (1995)	GX-19320	wood	0.365 $\pm$ 0.090	1494, 1601, 1616	1410–1954
	GX-19324	twigs	0.190 $\pm$ 0.095	1674, 1779, 1801, 1943, 1954	1488–1955
tii (1963–66)	GX-19325	wood	0.635 $\pm$ 0.080	1319, 1369, 1386	1259–1438
	GX-19321	twigs	153.8 $\pm$ 1.5 PMC	1963 or 1969	na
	GX-19322	twigs	141.1 $\pm$ 1.1 PMC	1962 or 1974	na
rcw (1993)	GX-19323	twigs	127.7 $\pm$ 1.3 PMC	1959, 1961, or 1981	na
tij (1995)	GX-20788	twigs	117.5 $\pm$ 1.0 PMC	1958, 1995	na

All  $^{14}\text{C}$  analyses were performed by Geochron Laboratories. The raw dates are in years before 1950 (years BP), except for those labelled with PMC (percentage of modern carbon), which are post-1950. All raw values are  $\pm 1$  standard deviation (1  $\sigma$ ). Calendar age and 2  $\sigma$  range are calculated using the calibration curves presented in Stuiver and Becker (1993) and incorporated in a computer program (Stuiver and Reimer, 1993). The range in age for post-1950  $^{14}\text{C}$  ages is very small. Not applicable (na).

technique. It is possible that the cosmogenic ages of these boulders, on the order of 600 years or more, may be the correction that needs to be applied to the older fan surfaces for cosmogenic  $^3\text{He}$  inherited from a previous exposure history, or they may illustrate the consequences of exceeding the analytical bounds of the  $^3\text{He}_c$  technique.

### 3.1.7. $^{14}\text{C}$ analyses of historic debris-flow surfaces

Using repeat photography, Webb et al. (1996) dated five historic debris flow deposits, and they witnessed a 1995 event.  $^{14}\text{C}$  analyses of driftwood associated with these debris flows indicated a substantial residence time for organic debris in the drainage (Table 3). Driftwood collected from historic debris-flow levees was dated using radiocarbon to determine the association of organic material with the date of the debris flow that transported it. Driftwood on top of the 1939 deposit yielded a calendar date range of AD 1327–1638 (Table 3). Three samples of driftwood and twigs on the 1955 deposit correspond to calendar age ranges of AD 1259–1438, 1410–1954, and 1488–1955, respectively. Two samples of twigs from undifferentiated 1963/1966 deposits provided  $^{14}\text{C}$  activities that correspond to calendar dates of AD 1963 or 1969 and 1962 or 1974, respectively. Driftwood deposited by the 1993 flood and the 1995 debris flow had post-bomb  $^{14}\text{C}$  activities that correspond to calendar dates of AD 1959,

1961, or 1981 and 1958 or 1995, respectively (Table 3). Therefore, wood transported in debris flows can be as much as 600 years older than the event, and event post-bomb  $^{14}\text{C}$  estimates may deviate considerably from the year of the debris flow.

The  $^{14}\text{C}$  analyses from historic debris flows suggest that organic materials rarely purged from Prospect Canyon. The 1939 and 1955 debris flows transported wood that was significantly older than the known date of the transporting debris flow. This is expected; Ferguson (1971) found persistence of driftwood for as long as a thousand years along the mainstem Colorado River, and Webb (1996) documented dead trees in Grand Canyon that remained standing for 400–500 years.  $^{14}\text{C}$  ages on prehistoric debris flows may be as much as 600 years older than the event. Although post-bomb radiocarbon dating has been reportedly reliable in past flood studies (Baker et al., 1985), our results confirm the unreliability of some types of organic debris in post-bomb  $^{14}\text{C}$  analyses (Ely et al., 1992). Because  $^{14}\text{C}$  dates on recent debris flows are close to the known age of the deposit, we speculate that several debris flows may be required to flush most of the organic debris from the drainage. Moreover, in Prospect Canyon, the lag in association of the  $^{14}\text{C}$  age of organic material appear to be the same order of magnitude—500 to 1000 years—as the uncertainty in  $^3\text{He}_c$  age because of prior exposure.

Table 4  
 Characteristics of prehistoric and selected historic debris fans at the mouth of Prospect Canyon

Surface	Date of flood	Method of dating <sup>a</sup>	Maximum debris-fan area (ha)	Maximum debris-fan thickness (m)	Minimum debris-fan thickness (m)	Range in debris-fan volume (10 <sup>3</sup> m <sup>3</sup> )	Recurrence interval of volumes (years)	Constriction ratio (%)
tfa	1050 BC	<sup>3</sup> He	15.9 <sup>b</sup>	22	22	3,500	nc	100
tia	250 BC	<sup>3</sup> He	1.19 <sup>b</sup>	12	10	119–131	600	50
tib	250 BC	<sup>3</sup> He	2.23 <sup>b</sup>	20	15	335–446	2,000	100
tic–tie	nd	na	nc	nc	nc	100–400	1,500	nc
tif	AD 1434	<sup>14</sup> C	1.07 <sup>b</sup>	5.0	4.0	43–54	200	45
tig	AD 1939	<sup>3</sup> He, P, <sup>14</sup> C	1.25 <sup>b</sup>	5.0	3.5	44–63	200	80
–	AD 1954	P	0.42 <sup>c</sup>	2.0	1.6	3.2–8.4	15	40
tih	AD 1955	P, <sup>14</sup> C	0.73 <sup>c</sup>	2.9	2.1	15–21	60	70
tii	AD 1963	P, <sup>14</sup> C	0.73 <sup>y</sup>	1.9	1.7	12–14	40	60
–	AD 1966	P	0.38 <sup>y</sup>	1.6	1.0	3.8–6.1	15	35
tij	AD 1995	W	0.56	1.7	1.7	9.4	30	60

<sup>a</sup><sup>3</sup>He, cosmogenic <sup>3</sup>He; <sup>14</sup>C, radiocarbon dating; P, historical photography; W, witnessed.

<sup>b</sup>Area, volume, and constriction percentage were determined by projection of the slopes of remnant deposits into the Colorado River (Webb et al., 1996).

<sup>c</sup>Area, volume, and constriction percentage were determined by rectification of historical photographs (Webb et al., 1996).

All areas and volumes are for sediments exposed above a discharge of 140 m<sup>3</sup> s<sup>-1</sup>. Maximum thickness were estimated during field surveys of non-eroded debris flow deposits; minimum thickness are the thickness of debris-flow deposit that would cover immobile boulders at mouth of Prospect Creek. The maximum constriction is the percentage reduction in river width, compared with an average of upstream and downstream widths, at the narrowest part of the rapid (Webb et al., 1996). Not calculated (nc); not dated (nd); not applicable (na).

### 3.2. Magnitude and frequency of debris flows from Prospect Canyon

To estimate the frequency of debris flows from Prospect Canyon, we reconstructed the volumes of debris fans deposited by 11 debris flows (Table 4). Surface tfa (3 ka) has the largest area and volume of the underlying deposit. To obtain the most accurate volume for this surface, we added the volume of the entrenched channel and the volume of the projected debris-fan surface across the Colorado River to the volume that was surveyed in 1993. The reconstructed debris fan from surface tfa had an area of 16 ha and a reconstructed volume of  $3.5 \times 10^6 \text{ m}^3$  (Table 4). The 1939 debris flow, the largest historic event, deposited a debris fan of 1.25 ha and had a volume of  $44\text{--}63 \times 10^3 \text{ m}^3$ . The volumes of nine other debris flows ranged from 3.2 to  $446 \times 10^3 \text{ m}^3$  (Table 4).

The projected height indicates that the debris flow that deposited surface tfa crossed the Colorado River (Fig. 7). The height above the center of the river just above Lava Falls at a stage of  $140 \text{ m}^3 \text{ s}^{-1}$  was 19.3 m, which combined with the current depth of the channel, yields a maximum thickness of 30 m (Webb et al., 1996). The average thickness of the deposit that comprises surface tfa was about 22 m (Table 4). Other debris fans ranged in average thickness from 1.6 to 20 m (Table 4).

We combined the age-dating information with the volume data to estimate the frequency of debris flows from Prospect Canyon. We established a type I censored-data model with three censoring thresholds of debris-flow volume to reflect the known depositional and temporal data. The first threshold, at  $3 \times 10^6 \text{ m}^3$ , is based on surface tfa as the largest debris flow in the last 3 ka. The second threshold, at  $0.1 \times 10^6 \text{ m}^3$ , reflects the prehistoric inset surfaces, including surface tia through surface tif (Table 4) and had a time range of 2.2 ka. The final depositional threshold had a magnitude of  $3 \times 10^3 \text{ m}^3$ , a duration of 123 years, and represented the seven historical events. We did not use the 1435 AD radiocarbon dated sample in this analysis (surface tif). The latter threshold effectively reduces the problem of obliterative overlap of very small events and eliminates the problem of years with zero depositional volume.

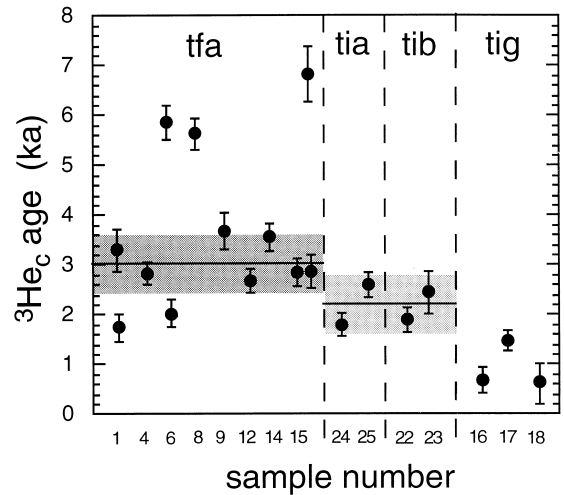


Fig. 7.  $^3\text{He}_c$  ages of debris fan boulders at Lava Falls, Grand Canyon. Surface tfa has two samples whose replicate analyses indicate that the  $^3\text{He}_c$  ages  $> 5$  ka for surface tfa are anomalous and should not be included in the average value for this surface. Samples from tfa are slightly older than surfaces tia and tib based on geometric relationships and this figure shows that the cosmogenic  $^3\text{He}_c$  ages indicate an age slightly younger for surfaces tia and tib than for surface tfa. Cosmogenic ages from surface tig (1939 AD debris flow) indicate that inheritance of cosmogenic  $^3\text{He}$  may cause an offset of a several hundred years for these debris flow samples.

The recurrence intervals for the debris fans (Table 4) provide a magnitude–frequency relation for historic debris flows from Prospect Canyon. Small historic debris flows, such as the 1995 event, have recurrence intervals of 15–60 years. The 0.5 ka and 1939 debris flows are 200-year events. Surface tia, the oldest of the inset surfaces, has a recurrence interval of 600 years, and surfaces tib and tic–tie have recurrence intervals of 2000 and 1500 yrs, respectively (Table 4). Surface tfa, which is an order of magnitude larger than the second largest debris flow, had a recurrence interval in excess of 10,000 years; therefore, we do not report a recurrence interval for this event. The standard error of the volume for recurrence intervals of 100–1000 years is 25–30%. To understand the effect of dating uncertainty, we varied the length of the first threshold between 3.0 ka and 3.6 ka, and we found that the volumes calculated for the 10-, 100-, and 1000-year recurrence intervals were nearly identical and well within the standard error of estimate.

### 3.3. Constrictions of the Colorado River

Constrictions of the Colorado River at the Prospect debris fan ranged from 35 to 100% (Table 4). Historically, the constriction has been less than or equal to 80%, with the greatest constriction occurring in 1939. At least two late Holocene debris flows from Prospect Canyon crossed and dammed the river. Other flows, such as the ones creating surfaces *tia* and *tif*, resulted in constrictions of about 50%. From the slope of the remnant deposits, we surmise that the apparent viscosity of these debris flows was higher than the others, leading to a steeper slope on the debris fan. Alternatively, these flows may have occurred on a wider debris fan, causing the flow to begin deceleration and deposition higher on the debris fan with less deposition and constriction in the river.

## 4. Conclusions

Using  $^3\text{He}_c$  and  $^{14}\text{C}$  dating, combined with historical repeat photography, we determined absolute ages for late Holocene debris-flow surfaces on the Prospect Canyon debris fan in Grand Canyon. We then calculated recurrence intervals for the volume of debris flows using the age-dating data to constrain the temporal range of deposition. These recurrence intervals indicate that small debris flows, such as the 1995 event, occur relatively frequently in Prospect Canyon, and that large, fan-forming debris flows recur at a frequency of several hundred to several thousand years. The uncertainty in age-dating techniques only adds slightly to the uncertainty in recurrence intervals and suggests that a robust magnitude-frequency model for late Holocene debris flows can be based on a combination of dating techniques.

The largest debris flow, which corresponds to surface *tfa*, has a recurrence interval in excess of 10,000 years, which implies an unusual size for the event. Melis et al. (1994) speculate that the initiation of debris flows is related to the occurrence of faults in tributary canyons and the amount of available talus. Jackson (1990) reports that the Toroweap Fault is the most active fault in Arizona, and its most recent large earthquake occurred 3 ka and had a

magnitude of 7.1 to 7.2 on the Richter scale. Such an earthquake would produce abundant talus in Prospect Canyon for an unusually large debris flow, if sufficient run-off occurred. In a study of ephemeral lakes west of Prospect Canyon, Enzel (1992) and Enzel et al. (1989) found deposits indicative of a persistent lake; one  $^{14}\text{C}$  date indicates the lake formed about 3.6 ka under persistent atmospheric-circulation patterns that would spawn unusually large, winter floods. Given the lag between  $^{14}\text{C}$  age and the transporting event, the same storms causing persistent lakes in the Mojave Desert could have initiated large debris flows in Prospect Canyon.

The  $^3\text{He}_c$  dating technique is valid for debris flows carrying olivine-laden basalts as young as a few thousand years, but uncertainty exists about corrections for previous exposure history and a small amount of inherited radiogenic  $^4\text{He}$ . Because of these uncertainties, a brute force approach might be used where many different samples are analyzed instead of one or two samples, as is typically collected from older exposure surfaces and those with 'single-event' histories. Despite these problems, we conclude that the three major debris fan surfaces in the Prospect debris complex, surfaces *tfa*, *tfb*, and *tia*, have integrated exposure ages of about  $3.0 \pm 0.6$ ,  $2.2 \pm 0.4$ , and  $2.2 \pm 0.6$  ka. These integrated exposure ages are maximum ages because of the problem of previous exposure, and the true age of emplacement may be a few hundred years younger than those given, but probably within the stated uncertainty.  $^{14}\text{C}$  analysis of debris flow deposits also is likely to overestimate the age of debris flow events because wood persists for up to several hundred years in these drainages.

## Acknowledgements

We thank Steve Eudaley, Diane Grua, Terry Maresca, Marker Marshall, Travis McGrath, Rachel Sobrero, Jessica Stewart, Mike Taylor, S. Tharnstrom, and Toni Yocum for their valued field assistance. Jan Bowers, Peter Griffiths, Mimi Murov, Betsy Pierson, Kate Thompson, and Kelly Burke contributed valuable technical expertise to this project. Mia Hanson's assistance contributed greatly to all aspects of the project work. Betsy Menand con-

tributed drawings of stratigraphic sections. The following professional river guides and support personnel contributed their boating skills and knowledge of the river: Gary Bolton, Kenton Grua, Bob Grusy, Les Hibbert, and Kelly Smith. Special thanks to Frank Protiva, Chris Brode, and Mark Gonzales of the GCES survey staff for assistance in estimating areas and volumes for the Prospect Canyon debris fan. We give special thanks to Dave Wegner, the former program manager for GCES, for funding our research. The cosmogenic component of this study was funded by the National Science Foundation.

## References

- Baker, V.R., Pickup, G., Polach, H.A., 1985. Radiocarbon dating of flood events, Katherine Gorge, Northern Territory, Australia. *Geology* 13, 344–347.
- Billingsley, G.H., Jr., Huntoon, P.W., 1983. Geologic map of Vulcans Throne and vicinity, western Grand Canyon, Arizona: Grand Canyon, Arizona, Grand Canyon Natural History Association Map, scale 1:62,500, 1 sheet.
- Birkeland, P.W., 1984. *Soils and Geomorphology*. Oxford Univ. Press, New York, 372 p.
- Bowers, J.E., Webb, R.H., Pierson, E.A., 1998. Primary succession of desert plants on debris-flow terraces, Grand Canyon, Arizona, USA, *J. Arid Environ.*, in press.
- Cerling, T.E., 1990. Dating geomorphic surfaces using cosmogenic  $^3\text{He}$ . *Quat. Res.* 33, 148–153.
- Cerling, T.E., Craig, H., 1994a. Geomorphology and in situ cosmogenic isotopes. *Annu. Rev. Earth Planet. Sci.* 22, 273–317.
- Cerling, T.E., Craig, H., 1994b. Cosmogenic  $^3\text{He}$  production rates from 39°N to 46°N latitude, western USA and France. *Geochim. Cosmochim. Acta* 58, 249–255.
- Cerling, T.E., Poreda, R.J., Rathburn, S.L., 1994. Cosmogenic  $^3\text{He}$  and  $^{21}\text{Ne}$  age of the Big Lost River flood, Snake River Plain, Idaho. *Geology* 22, 227–230.
- Costa, J.E., 1984. Physical geomorphology of debris flows. In: Costa, J.E., Fleisher, P.J. (Eds.), *Developments and Applications of Geomorphology*. Springer-Verlag, Berlin, p. 268–317.
- Craig, H., Poreda, R.J., 1986. Cosmogenic  $^3\text{He}$  in terrestrial rocks: the summit lavas of Maui. *Proc. Natl. Acad. Sci. USA* 83, 1970–1974.
- Ely, L.L., Webb, R.H., Enzel, Yehouda, 1992. Accuracy of post-bomb  $^{137}\text{Cs}$  and  $^{14}\text{C}$  in dating fluvial deposits. *Quat. Res.* 38, 196–204.
- Enzel, Y., 1992. Flood frequency of the Mojave River and the formation of late Holocene playa lakes, southern California, USA. *Holocene* 2, 11–18.
- Enzel, Y., Cayan, D.R., Anderson, R.Y., Wells, S.G., 1989. Atmospheric circulation during Holocene lake stands in the Mojave Desert: evidence of regional climate change. *Nature* 341, 44–47.
- Ferguson, C.W., 1971. Tree-ring dating of Colorado River driftwood in the Grand Canyon. *Arizona Acad. Sci.* 1, 351–366.
- Gibbons, A.B., Megeath, J.E., Pierce, K.L., 1984. Probability of moraine survival in a succession of glacial advances. *Geology* 12, 327–330.
- Graf, W.L., 1979. Rapids in canyon rivers. *J. Geol.* 87, 533–551.
- Griffiths, P.G., Webb, R.H., Melis, T.S., 1996. Initiation and frequency of debris flows in Grand Canyon, Arizona, US Geol. Survey Open-File Report 96-491, 35 p.
- Hamblin, W.K., 1994. Late Cenozoic lava dams in the western Grand Canyon. *Geol. Soc. Am. Mem.*, 183, 139 p.
- Hamblin, W.K., Rigby, J.K., 1968. Guidebook to the Colorado River: I. Lee's Ferry to Phantom Ranch in Grand Canyon National Park. *Brigham Young Univ. Geol. Studies* 15 (5), 84.
- Hammack, L., Wohl, E., 1996. Debris-fan formation and rapid modification at Warm Springs Rapid, Yampa River, Colorado. *J. Geol.* 104, 729–740.
- Hereford, R., 1996. Map showing surficial geology and geomorphology of the Palisades Creek area, Grand Canyon National Park, Arizona, US Geol. Surv. Misc. Invest. Series Map I-2449, scale 1:2000.
- Hereford, R., Thompson, K.S., Burke, K.J., Fairley, H.C., 1996. Tributary debris fans and the late Holocene alluvial chronology of the Colorado River, eastern Grand Canyon, Arizona. *Geol. Soc. Am. Bull.* 108, 3–19.
- Howard, A., Dolan, R., 1981. Geomorphology of the Colorado River in Grand Canyon. *J. Geol.* 89, 269–297.
- Jackson, G.W., 1990. The Toroweap fault—one of the most active faults in Arizona. *Arizona Geology* 20, 7–10.
- Jackson, L.E. Jr., 1977. Dating and recurrence frequency of prehistoric mudflows near Big Sur, Monterey County, California. *J. Res. US Geol. Surv.* 5, 17–32.
- Johnson, A.M., Rodine, J.R., 1984. Debris flow. In: Brunsten, D., Prior, D.B. (Eds.), *Slope Instability*. Wiley, New York, pp. 257–361.
- Kieffer, S.W., 1987. The rapids and waves of the Colorado River, Grand Canyon, Arizona, US Geol. Surv. Open-File Report 87-096, 69 p.
- Kieffer, S.W., 1988. Hydraulic map of Lava Falls Rapid, Grand Canyon, Arizona, US Geol. Surv. Misc. Invest. Series, Map I-1897-J, scale 1:1000, 1 sheet.
- Kite, G.W., 1988. Frequency and risk analyses in hydrology. *Water Resources Publications*, Littleton, Colorado, 257 p.
- Klein, J., Giegengack, R., Middleton, R., Sharma, P., Underwood, J.R., Weeks, R.A., 1986. Revealing histories of exposure using in situ-produced  $^{26}\text{Al}$  and  $^{10}\text{Be}$  in Libyan desert glass. *Radiocarbon* 28, 547–555.
- Kochel, R.C., 1987. Holocene debris flows in central Virginia. *Rev. Eng. Geol.* 7, 139–155.
- Kurz, M.D., 1986. Cosmogenic helium in a terrestrial igneous rock. *Nature* 320, 435–439.
- Lal, D., 1988. In situ-produced cosmogenic isotopes in terrestrial rocks. *Annu. Rev. Earth Planet. Sci.* 16, 355–388.
- Lal, D., Craig, H., Wacker, J.F., Poreda, R., 1989.  $^3\text{He}$  in

- diamonds: the cosmogenic component. *Geochim. Cosmochim. Acta* 53, 569–574.
- Lips, E.W., Wieczorek, G.F., 1990. Recurrence of debris flows on an alluvial fan in central Utah. In: *Hydraulics/Hydrology of Arid lands: Proceedings of the International Symposium, Hydraulics and Irrigation Divisions, American Society of Civil Engineers*, pp. 555–560.
- Machette, M.N., 1985. Calcic soils of the southwestern United States, *Geol. Soc. Am. Spec. Paper* 203, pp. 1–21.
- Meyer, G.A., Wells, S.G., Jull, A.J.T., 1995. Fire and alluvial chronology in Yellowstone National park—climatic and intrinsic controls on Holocene geomorphic processes. *Geol. Soc. Am. Bull.* 107, 1211–1230.
- Melis, T.S., Webb, R.H., Griffiths, P.G., Wise, T.J., 1994. Magnitude and frequency data for historic debris flows in Grand Canyon National Park and vicinity, Arizona, *US Geol. Surv. Water Res. Invest. Report* 94-4214, 285 p.
- Nash, R.F., 1989. The big drops, ten legendary rapids of the American west. Johnson Books, Boulder, Colorado, 216 p.
- Nishiizumi, K., Lal, D., Klein, J., Middleton, R., Arnold, J.R., 1989. Cosmic ray production rates of  $^{10}\text{Be}$  and  $^{26}\text{Al}$  in quartz from glacially polished rocks. *J. Geophys. Res.* 94, 17907–17915.
- Osterkamp, W.R., Hupp, C.R., 1987. Dating and interpretation of debris flows by geologic and botanical methods at Whitney Creek gorge, Mount Shasta, California. *Rev. Eng. Geol.* 7, 157–163.
- Péwé, T.L., 1968. *Colorado River Guidebook*, Lees Ferry to Phantom Ranch. Privately published, Tempe, Arizona, 78 p.
- Poreda, R.J., Cerling, T.E., 1992. Cosmogenic neon in recent lavas from the western United States. *Geophys. Res. Lett.* 19, 1863–1866.
- Poreda, R.J., Farley, K.A., 1992. Rare gases in Samoan xenoliths. *Earth Planet. Sci. Lett.* 113, 129–144.
- Shlemon, R.J., Wright, R.H., Montgomery, D.R., 1987. Anatomy of a debris flow, Pacifica, California. *Rev. Eng. Geol.* 7, 181–199.
- Simmons, G.C., Gaskill, D.L., 1969. *River runner's guide to the canyons of the Green and Colorado Rivers, with emphasis on geologic features*, Vol. III, Marble Gorge and Grand Canyon. Northland Press, Flagstaff, Arizona, 132 p.
- Stedinger, J.R., Cohn, T.A., 1986. Flood frequency analysis with historical and paleoflood information. *Water Res.* 22, 785–793.
- Stedinger, J., Surani, R., Therivel, R., 1988. *MAX users guide*. Cornell University, Dept. Environ. Eng. Ithaca, NY.
- Stevens, L., 1990. *The Colorado River in Grand Canyon, A Guide*. Red Lake Book, Flagstaff, Arizona, 115 p.
- Stuiver, M., Becker, B., 1993. High-precision calibration of the radiocarbon time scale AD 1950–6000 BC. *Radiocarbon* 35, 35–65.
- Stuiver, M., Reimer, P.J., 1993. *CALIB user's guide for Macintosh computers*, Rev 3.0.3A. Univ. Washington, Quat. Res. Center, Seattle, Washington.
- Vasek, F.C., 1980. Creosote bush, long-lived clones in the Mojave Desert. *Am. J. Botany* 67, 246–255.
- Webb, R.H., 1996. Grand Canyon, a Century of Environmental Change: Rephotography of the 1889–1890 Stanton Expedition. University of Arizona Press, Tucson, Arizona, 290 p.
- Webb, R.H., Steiger, J.W., Turner, R.M., 1987. Dynamics of Mojave Desert shrub vegetation in the Panamint Mountains. *Ecology* 50, 478–490.
- Webb, R.H., Pringle, P.T., Reneau, S.L., Rink, G.R., 1988a. Monument Creek debris flow, 1984: implications for formation of rapids on the Colorado River in Grand Canyon National Park. *Geology* 16, 50–54.
- Webb, R.H., Steiger, J.W., Newman, E.B., 1988b. The response of vegetation to disturbance in Death Valley National Monument, California, *US Geol. Surv. Bull.* 1793, 103 p.
- Webb, R.H., Pringle, P.T., Rink, G.R., 1989. Debris flows from tributaries of the Colorado River, Grand Canyon National Park, Arizona, *US Geol. Surv. Prof. Paper* 1492, 39 p.
- Webb, R.H., Melis, T.S., Wise, T.W., Elliott, J.G., 1996. The great cataract, Effects of late Holocene debris flows on Lava Falls Rapid, Grand Canyon National Park and Hualapai Indian Reservation, Arizona, *US Geol. Surv. Open-file Report* 96-460, 96 p.